J. Fluid Mech. (1994), *vol.* 273, *pp.* 83–107

The nucleation, growth and settling of crystals from a turbulently convecting fluid

By RICHARD A. JARVIS[1]† AND ANDREW W. WOODS[2]

[1] Department of Geology and Geophysics, Yale University, New Haven, CT 06511, USA

[2] Institute of Theoretical Geophysics, Department of Applied Mathematics and Theoretical Physics, University of Cambridge, Silver Street, Cambridge CB3 9EW, UK

(Received 4 January 1993 and in revised form 3 February 1994)

We present a new model to describe the thermal and compositional evolution of a binary alloy which is cooled from above. Explicit account is taken of the nucleation of crystals in the cold upper thermal boundary layer, the growth of crystals in the turbulently convecting interior, and their subsequent gravitational settling to the floor of the chamber. The crystallization of one solid phase only is considered. When the residence time of a typical crystal within the convecting bulk is short compared with the overall cooling time of the fluid, the crystal size distribution loses memory of earlier conditions in the fluid and the number density simply decays exponentially with the cube of the crystal size. A quasi-steady state exists in which the rate of crystal production is balanced by the rate of sedimentation at the floor, allowing the volume fraction of suspended crystals to remain small until convection ceases to be vigorous.

We focus on the situation in which the latent heat released by solidification would far exceed the heat flux extracted through convection if the melt undercooling were maintained equal to the initial temperature difference applied at the cold upper boundary. In this case, either the growth or nucleation of crystals must be limited in order that the fluid continues to cool. Both the growth-limited and nucleation-limited regimes may develop during the cooling of an individual fluid body, depending upon the thermal boundary condition at the upper boundary of the convecting portion of the fluid.

We calculate how the mean crystal size within the sedimented crystal pile evolves as the fluid cools. During the growth-limited regime, the mean crystal size in the crystal pile typically decreases with height, owing to the decrease in the extracted heat flux and the greater efficiency of crystal settling as the fluid layer becomes shallower. In contrast, during the nucleation-limited regime, the fluid undercooling may increase significantly as the fluid cools, and inverse grading (large crystals over small) is possible. We discuss the possible application of our theory to the cooling of large igneous intrusions.

1. Introduction

The processes by which a hot, vigorously convecting body of fluid cools and solidifies have attracted much attention owing to their importance in the generation of igneous rocks (see the review by Huppert 1990), as well as in chemical processing (Randolph & Larson 1971). A central issue in igneous petrology concerns the

† Present address: Laboratoire de Dynamique des Systèmes Géologiques, Institut de Physique du Globe, 4 place Jussieu, 75252 Paris Cedex 05, France.

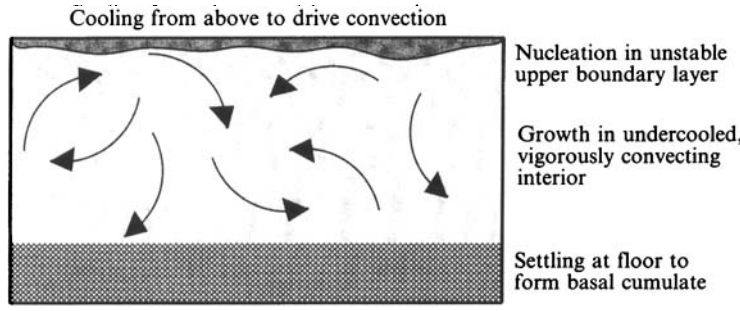

FIGURE 1. Schematic of a vigorously convecting fluid body driven by cooling from above. Crystals nucleate in the cold upper boundary layer, where the supercooling is greatest, before entering the bulk convecting fluid either by settling or by repeated boundary-layer instability. Within the vigorously convecting interior, crystals continue to grow until settling out at the base to form a cumulate pile.

mechanisms by which hot molten magma cools and solidifies to form large igneous intrusions. Much recent theoretical and experimental work on the interactions between convection and crystallization in vigorously convecting fluids has examined the growth of solid attached to the cooled boundaries (Brandeis, Jaupart & Allègre 1984; Woods & Huppert 1989; Kerr *et al.* 1990). However, recent experiments by Kerr *et al.* (1990) and Martin (1990) suggest that if the fluid becomes sufficiently supercooled, then some crystals may also nucleate and grow within the convecting body of fluid. As these crystals grow, they settle to the base of the fluid to form a crystal pile (figure 1). The idea that crystal settling may generate some features associated with igneous intrusions is not new (Bowen 1915; Bartlett 1969), and is still the focus of much debate in the petrological literature (for example Campbell 1978; Martin & Nokes 1989). However, to date, no complete model of the solidification process has been developed incorporating details of both the generation and settling of crystals, and the thermal and compositional history of the fluid.

The purpose of this paper is to develop and investigate such a model for the nucleation, growth and sedimentation of crystals in a binary fluid as it is cooled from above. We investigate how the crystallization dynamics interacts with the convective cooling of the fluid, and identify the processes which control the evolution of the mean size of suspended crystals as the system evolves. This lends insight into the mean grain size variation in the crystal pile. Our model is a synthesis of a model of the sedimentation of a dilute suspension of particles from a turbulently convecting fluid (Martin & Nokes 1989) and of simple theoretical models for the nucleation and growth of crystals in a supercooled fluid (e.g. Kirkpatrick 1976; Dowty 1980; Brandeis *et al.* 1984; Brandeis & Jaupart 1987; Spohn, Hort & Fischer 1988), combined with a general population dynamics representation for the crystal size distribution (Randolph & Larson 1971).

In §2, we shall briefly introduce the equations for the conservation of heat and mass in a turbulently convecting fluid cooled from above, followed in §3 by some general theory for the crystal size distribution based upon the nucleation and growth kinetics. For the present discussion, we shall consider the crystallization of only a single solid phase. We then analyse the quasi-steady form of this crystal distribution which applies when the cooling time of the fluid far exceeds the typical residence time of a crystal in the fluid (§4). In §5, we couple our quasi-steady model with the global model of heat and mass conservation of §2, introducing suitable dimensionless variables to facilitate our analysis. In §6, we identify two asymptotic regimes which govern the cooling of the

fluid in the limit that the heat released by the crystallization per unit time, based upon the initial undercooling, far exceeds the heat flux extracted from the fluid per unit time. We then examine (§7) the effect of different thermal boundary conditions at the roof upon the evolution of the fluid by studying selected illustrative examples. Finally, in §8, we discuss our results, with particular emphasis on geological applications.

2. Evolution of a fluid cooled from above

We study the cooling from above of a fluid body with small aspect ratio (depth/width). We shall treat fluids which can be characterized as a binary alloy, with distinct liquidus and solidus curves such that heavy crystals nucleate and grow within the fluid. Typically, the crystals formed differ in composition from the surrounding fluid. The effects of pressure variations upon the liquidus and solidus curves are neglected. We also neglect the effect of composition upon fluid density, and consider only thermally driven convection.

We suppose an initial state in which there are no crystals, and treat only cases in which the crystal volume fraction remains sufficiently small for fluid motions to be unaffected by the presence of the suspended crystals. As outlined below, sufficiently rapid settling of the dense crystals to form a basal cumulate can allow a low crystal volume fraction within the fluid throughout crystallization. We consider high-Prandtl-number fluids, in line with our preferred application to magmatic systems, and further restrict ourselves to cases in which the fluid is vigorously convecting, and hence well-mixed. For infinite-Prandtl-number convection in fluids of small aspect ratio, this requires Rayleigh number $Ra \gtrsim 10^7$, a constraint which may be relaxed by the presence of internal heating (Hansen, Yuen & Kroening 1992). The well-mixed assumption leads us to formulate our theory in terms of state variables which are spatially uniform, with the necessary exception of the thermal boundary layer adjacent to the cold roof. In particular, the main convecting portion of the fluid may be considered to have constant viscosity. However, the model described here is essentially nonlinear, and for less vigorous convection, it would be necessary to consider the combined effects of spatial variations in temperature, composition and crystal population.

We neglect post-cumulus processes, such as Ostwald ripening, and *in-situ* crystallization at the roof and the floor, which may lead to significant compositional convection in the interstices under some circumstances (see, for example, Tait & Jaupart 1992). Instead, we focus on the initial formation of the cumulate pile and assume for simplicity that the crystal cumulate is perfectly packed, with no interstitial fluid.

First, we shall describe the overall heat and mass balances applicable to the crystallization of a fluid cooled from above. When the fluid body is cooled from above, the extracted heat flux is balanced by a combination of heat loss from the fluid through the roof and the release of latent heat when crystals are formed. If the temperature of the bulk convecting fluid is T, then

$$(H-h)\rho c_p \frac{\mathrm{d}T}{\mathrm{d}t} = -\mathscr{F} + \rho \mathscr{L}(H-h) R_P, \tag{2.1}$$

in which ρ is the fluid density, c_p its thermal capacity, $\mathscr{L}$ is the latent heat of crystallization released per unit mass of fluid, and $\mathscr{F}$ is the heat flux per unit area through the roof of the chamber. The volume of new solid formed in unit time per unit volume is R_P and the thickness of the convecting fluid layer is $(H-h)$, where H is its

initial thickness and h is the thickness of the cumulate pile at the floor. The rate of growth of a perfectly packed cumulate is given by

$$\mathrm{d}h/\mathrm{d}t = R_S, \tag{2.2}$$

where R_S is the crystal sedimentation rate. In writing (2.1), we have assumed that the basal cumulate is perfectly insulated, and retains its temperature from the time of sedimentation. An alternative limiting case could be a perfectly conducting cumulate which remains at the same temperature as the overlying fluid at all times, for which the factor $(H-h)$ on the left-hand side of (2.1) would simply become equal to H.

For vigorously convecting fluids, heat transfer is effected by successive episodes of diffusive growth of a thermal boundary layer, followed by detachment of plumes when this boundary layer becomes unstable (Howard 1964). If the fluid body is sufficiently large, the heat flux extracted is independent of the overall thickness of the fluid layer, and can be related to the temperature T_R of the roof by the expression (Turner 1979)

$$\mathscr{F} = \rho c_p J(T-T_R)^{\frac{4}{3}}, \tag{2.3}$$

where

$$J \sim 0.16(g\alpha\kappa^2/\nu)^{\frac{1}{3}} \tag{2.4}$$

for convection driven only by cooling from above (Katsaros *et al.* 1977). Here, g is the acceleration due to gravity, α is the thermal expansion coefficient, κ is thermal diffusivity, and ν is the kinematic viscosity of the fluid. The upper boundary layer has scale thickness

$$h_b = \rho c_p \kappa(T-T_R)/\mathscr{F} \sim 6.4Ra^{-\frac{1}{3}}(H-h), \tag{2.5}$$

where $Ra = g\alpha(T-T_R)(H-h)^3/\nu\kappa$ is the Rayleigh number. Note that h_b is independent of the fluid depth $(H-h)$.

Conservation of mass in the bulk convecting fluid takes the form

$$(1-\Phi)\,\mathrm{d}C/\mathrm{d}t = (C-C_s)\,R_P, \tag{2.6}$$

where C is the composition of the bulk convecting fluid, C_s the composition of the solid formed, and Φ the volume fraction of suspended crystals within the fluid.

We assume here that only one crystalline phase is formed, which for a eutectic binary alloy requires the fluid temperature to be above the eutectic temperature T_E. If the liquidus, $T_L(C)$, and solidus curves can be considered to be locally linear, with liquidus slope $T_L' = m$ and distribution coefficient k_D $(0 \leqslant k_D < 1)$, then the solid composition C_s and liquidus temperature T_L are related to the fluid composition C by the expressions

$$C_s - C_\alpha = k_D(C-C_\alpha); \tag{2.7}$$

$$T_L = T_\alpha + m(C-C_\alpha), \tag{2.8}$$

where (T_α, C_α) represents the point on the phase diagram at which the solidus and liquidus curves intercept (figure 2) and $T_\alpha \geqslant T_L$. The mass conservation equation (2.6) can then be written as an evolution equation for the liquidus temperature of the fluid,

$$\mathrm{d}T_L/\mathrm{d}t = -(1-k_D)(T_\alpha - T_L)\,R_P, \tag{2.9}$$

assuming that $\Phi \ll 1$. A similar expression may be obtained for a general liquidus relation $T_L(C)$ and non-constant distribution coefficient $k_D(C)$.

To complete the above model, we require the crystal production and sedimentation rates, R_P and R_S, and the roof temperature, T_R. We calculate R_P and R_S in the following two sections, but, in general, the roof temperature T_R can only be determined by coupling the thermal evolution of the convecting fluid body to a model for the

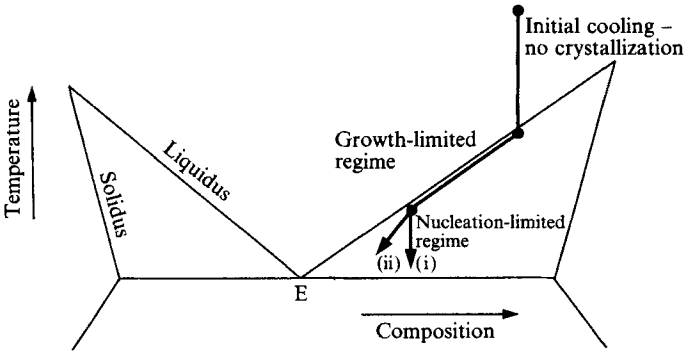

FIGURE 2. Typical eutectic equilibrium phase diagram with eutectic point marked E. Above the liquidus temperature, the binary alloy is liquid at equilibrium, while below the solidus it is solid. The general evolution of the bulk convecting fluid as it is cooled from above is given by the bold line. First, the fluid is cooled to its liquidus temperature, at which time the crystals nucleated in the cold upper boundary layer may continue to grow in the interior. The continual release of latent heat maintains the bulk fluid temperature just below the liquidus until the undercooling in the upper boundary layer becomes too small for significant nucleation to continue. Thereafter, the crystal population is characterized by a smaller number of larger crystals and the undercooling within the bulk convecting interior increases. If the roof temperature is constant, this final phase is not associated with any cumulate growth, (i), and the fluid composition remains constant. If, however, the roof temperature is decreasing the liquidus temperature may continue to decrease, (ii), and there is a finite cumulate thickness associated with the nucleation-limited regime.

overlying region, this may be solid (melting or freezing), or a stagnant viscous lid which caps the convecting part of the fluid when there is a strong viscosity variation between fluid in the interior and the fluid adjacent to the cold upper boundary (Richter 1978; Jaupart & Parsons 1985; Bruce 1989; Davaille & Jaupart 1993). In these cases, the 'roof' of the chamber should be understood to be coincident with the top of the mobile, convectively unstable part of the fluid. However, in this paper, we will be interested only in the evolution of the fluid part of the system, and shall not constrain ourselves to any specific models for the roof region. After a general discussion in §6, we shall treat two simple examples designed to demonstrate the fundamental physical balances and to illustrate the possible range of qualitative behaviours.

3. Crystal nucleation, growth and settling

New crystals can nucleate and grow wherever the constitutional undercooling in the fluid is sufficiently large. Nucleation does not occur immediately the fluid temperature falls below the liquidus, but only when the undercooling exceeds a critical value, termed the nucleation delay (Dowty 1980). Hence, for a fluid cooled from above, nucleation occurs first within the cold upper boundary layer (Brandeis *et al.* 1984). Moreover, we shall see in §5 below that under suitable conditions, the undercooling within the convecting bulk of the fluid remains below the critical nucleation delay, in which case significant nucleation of free crystals is restricted to the upper boundary layer at all times.

After nucleation, crystals are extracted from the cold upper boundary layer, either by settling or by entrainment in the cold downgoing plumes (Brandeis & Jaupart 1986; Sparks *et al.* 1993), depending upon the frequency of plume events: for convection at sufficiently high Rayleigh number, crystals are typically advected out by plumes before they have grown sufficiently large to settle out by themselves (see Appendix A).

Whichever mechanism applies, we assume here for simplicity that the mean crystal radius upon extraction from the boundary layer is much less than the mean radius of sedimented crystals. In other words, we assume that growth occurs predominantly while the crystals are suspended within the main body of convecting melt. This enables us to treat nucleation as occurring simultaneously with extraction.

Once entrained into the main body of convecting melt, crystals remain suspended and grow until they settle out at the base of the fluid body. For sufficiently vigorous convection, i.e. when the mean vertical fluid velocity far exceeds the Stokes settling velocity for individual crystals, the crystal population may be considered well-mixed, and hence spatially uniform (Martin & Nokes 1989). For a dilute ($\Phi \ll 1$) uniform suspension of particles in a turbulently convecting fluid, Martin & Nokes (1988, 1989) have determined experimentally and theoretically that the rate of sedimentation is described by an exponential decay law based upon the Stokesian settling velocities of the particles. Sedimentation occurs as particles pass through the thin viscous boundary layer at the base of the convecting region (Turner, Huppert & Sparks 1986; Martin & Nokes 1989). This description may be also be applied to the settling of suspended crystals if the crystal population is sufficiently dilute for the thermal convection to be unaffected, and if the crystals may be considered passive tracers within the convecting interior, above the basal viscous boundary layer. The validity of this passive-tracer assumption is examined further in Appendix B.

3.1. *The crystal size distribution function*

To describe the mean crystal population in the convecting interior, we define a crystal size distribution function $\phi(a,t)$ such that, at time t there are $\phi(a,t)\,\mathrm{d}a$ crystals with radius between a and $a+\mathrm{d}a$ per unit volume of the chamber. As outlined above, these crystals have been generated within the cold upper boundary layer and entrained into the bulk convective flow, where they grow before sedimentation. We assume for simplicity that the crystals are spherical. Following Martin & Nokes (1989), the rate of sedimentation of crystals of radius a is $W_S\phi/(H-h)$, where $W_S(a) = 2g'a^2/9\nu$ is the Stokes settling velocity for an unhindered sphere of radius a, and $g' = g\Delta\rho/\rho$ is the reduced gravity associated with crystals of density $\rho+\Delta\rho$ settling out of fluid of density ρ. If the radii of the crystals grow at a rate $V(t)$, where $V(t)$ reflects the fluid conditions at time t, then the number of crystals of radius a evolves according to the equation (cf. Randolph & Larson 1971; Marsh 1988)

$$\frac{\partial\phi}{\partial t}+\frac{\partial(V\phi)}{\partial a} = -\frac{\lambda a^2}{H-h}\phi, \tag{3.1}$$

where $\lambda = 2g'/9\nu$. We assume that the crystal growth rate V is independent of the crystal radius a. Note that the kinematic viscosity ν is in general a function of the fluid temperature and crystal content.

Initially there are no crystals, and so (3.1) has initial condition $\phi(a,0) = 0$. The rate of nucleation of new crystals per unit chamber volume is $N(t)$, which gives the additional boundary condition $\phi(0,t) = N(t)/V(t)$ (see Appendix C). Hence, solving along characteristics, the general solution to (3.1) is

$$\phi(a(t_0;t),t) = \frac{N(t_0)}{V(t_0)}\exp\left(-\int_{t_0}^{t}\frac{\lambda(t')\,a^2(t_0;t')}{H-h(t')}\,\mathrm{d}t'\right), \tag{3.2}$$

$$a(t_0;t) = \int_{t_0}^{t} V(t')\,\mathrm{d}t', \tag{3.3}$$

in which $t_0 \geqslant 0$ is the time of nucleation for crystals which have radius a at time t. From the crystal distribution, we may obtain the rate of production R_P of new solid per unit volume and the crystal sedimentation rate R_S,

$$R_P(t) = 4\pi V(t) \int_0^{a(0;t)} a^2 \phi(a, t)\, \mathrm{d}a; \tag{3.4}$$

$$R_S(t) = \tfrac{4}{3}\pi\lambda(t) \int_0^{a(0;t)} a^5 \phi(a, t)\, \mathrm{d}a, \tag{3.5}$$

where $a(0;t)$ is the maximum crystal radius at time t. In addition, the overall crystal fraction, Φ, and the average radius $\bar{a}_d$ of sedimented crystals, are

$$\Phi(t) = \tfrac{4}{3}\pi \int_0^{a(0;t)} a^3 \phi(a, t)\, \mathrm{d}a; \tag{3.6}$$

$$\bar{a}_d(t) = \int_0^{a(0;t)} a^3 \phi(a, t)\, \mathrm{d}a \Big/ \int_0^{a(0;t)} a^2 \phi(a, t)\, \mathrm{d}a. \tag{3.7}$$

In defining $\bar{a}_d$, we have taken a simple numerical average, with the additional factor a^2 reflecting the faster settling rates of larger crystals. We shall use (3.6) in Appendix D below to confirm under what conditions our assumption of a small crystal volume fraction is valid.

3.2. *Nucleation and growth rates*

For a binary alloy, the rates of nucleation and growth of crystals are typically modelled as dependent only upon the locally averaged constitutional undercooling $(T_L - T)$ (Kirkpatrick 1976; Dowty 1980; Brandeis *et al.* 1984). In the present context, this requires mixing of the bulk fluid to be sufficiently intense for crystallization not to be suppressed by the growth of diffusive compositional boundary layers around individual crystals. Above the eutectic temperature (if it exists), just one crystalline phase nucleates, and only then if the fluid is supercooled sufficiently. This phase typically takes the form of a solid solution, in which molecules of one component are included within a crystalline matrix of the second, dominant component. For a eutectic binary alloy, the choice of dominant component depends upon which side of the eutectic composition the fluid composition lies.

When a eutectic binary alloy is cooled below the eutectic temperature, however, the second crystalline phase is able to grow within the interior. This can lead to some rich dynamics in the neighbourhood of the eutectic point when a stagnant (or completely uniform) fluid body is cooled. For example, in the model of Hort & Spohn (1991) for the completely uniform cooling of a fluid body, oscillatory nucleation of the two phases occurs, with the fluid composition and temperature evolving along a complex trajectory around the eutectic point. The evolution of two separate crystallising phases, each with their own kinetic laws and settling rates, is a complex and interesting problem, but before studying this case, it is sensible first to understand the settling dynamics of a single phase. Therefore, we shall here only treat crystallization above the eutectic temperature, which necessarily means that we cannot describe the entire solidification of the body when the roof is maintained below the eutectic temperature.

We now determine appropriate forms for the crystal nucleation and growth rates. We have argued that crystal nucleation occurs within the cold upper boundary layer, across which the fluid composition is approximately constant, since any compositional boundary layer would be much thinner than the outer thermal boundary layer.

Consequently, the appropriate undercooling for the nucleation process is $(T_L - T_R)$, where T_L is the liquidus temperature of the bulk fluid and T_R is the roof temperature. In addition, the nucleation rate must be proportional to $h_b/(H-h)$, where h_b is the scale thickness of the upper boundary layer and $(H-h)$ is the depth of the convecting fluid layer. This multiplicative factor is necessary because crystals formed in the thin boundary layer are entrained into the convecting bulk and mixed throughout a greater volume. Hence, the nucleation rate N per unit chamber volume has the following functional form:

$$N(t) \equiv \frac{Bh_b(t)}{H-h(t)} \tilde{N}(T_L - T_R), \tag{3.8}$$

where $\tilde{N}(U)$ is the rate of nucleation per unit volume for a fluid with uniform constitutional undercooling U and $B \sim O(1)$ is a undetermined dimensionless constant, dependent upon the detailed structure of the thermal boundary layer. Here, we shall assume that $B = 1$.

In our model, crystal growth occurs predominantly within the convecting interior, whose undercooling is $(T_L - T)$. Therefore, the growth rate V has functional form

$$V(t) \equiv V(T_L - T). \tag{3.9}$$

In this paper, we shall not attempt to determine the precise form of the nucleation and growth rate functions $\tilde{N}$ and V by reference to attachment or diffusion kinetics, neither shall we require that nucleation be homogeneous or heterogeneous. Instead, we shall simply study parametric forms for dimensionless nucleation and growth rates as defined in § 5.1 below, thereby enabling the examination of a wide variety of (nonlinear) nucleation and growth behaviours.

4. Crystal residence time and the quasi-steady state

The model outlined in §§ 2 and 3 simplifies greatly when the typical residence time of a crystal within the convecting bulk is much shorter than the overall cooling timescale of the fluid.

From the heat conservation equation (2.1), the convective cooling timescale t_c is

$$t_c \sim (H-h)\rho c_p (T - T_R)/\mathscr{F}, \tag{4.1}$$

while the form of the exponential in the solution (3.2), (3.3) for the crystal size density function $\phi(a, t)$ suggests that the crystals remain in suspension for a time of order

$$t_{res} \sim [(H-h)/(\lambda V^2)]^{\frac{1}{3}}. \tag{4.2}$$

If $t_c \gg t_{res}$, then over the shorter crystal residence timescale, t_{res}, we may consider λ, V and N to be effectively constant, since these bulk properties evolve only over the longer fluid cooling timescale, t_c. This is termed the quasi-steady limit. However, the appropriateness of this limit cannot immediately be determined for a given set of kinetic laws and externally imposed conditions, because of the strong coupling between cooling and crystallization. Therefore, we first assume that $t_c \gg t_{res}$, and only later shall we determine conditions under which this approximation is valid (see Appendix D).

In the quasi-steady limit, we can solve (3.1) for the instantaneous crystal size distribution by taking the steady-state limit $(\partial/\partial t = 0)$. To see this formally, let us rewrite (3.3) in the form

$$a(t_0; t) = V(t_0)(t - t_0) + \tfrac{1}{2}(\mathrm{d}V/\mathrm{d}t)(t - t_0)^2 + \ldots. \tag{4.3}$$

Over a timescale $(t-t_0) = O(t_{res})$, the term $(t-t_0)\,\mathrm{d}V/\mathrm{d}t$ has magnitude $V\delta$, where $\delta = t_{res}/t_c \ll 1$. Thus,

$$a(t_0; t) = V(t)(t-t_0)(1+O(\delta)). \tag{4.4}$$

Similarly, we can form expansions for λ and N, which upon substitution into (3.2), give the result

$$\phi(a(t_0; t), t) = \frac{N(t_0)}{V(t_0)}(1+O(\delta))\exp\left[-\frac{\lambda(t)}{3(H-h(t))}V(t)^2(t-t_0)^3(1+O(\delta))\right] \tag{4.5}$$

for times $(t-t_0) = O(t_{res})$. This has the leading-order form

$$\phi(a, t) = \frac{N(t)}{V(t)}\exp\left[-\frac{\lambda(t)\,a^3}{3(H-h(t))\,V(t)}\right], \tag{4.6}$$

which is the same as the steady-state solution ($\partial/\partial t \equiv 0$) to (3.1). Note that for $a \gg Vt_{res}$, the exponential term in (4.6) becomes vanishingly small. Therefore, for $t \gg t_{res}$, integrals with respect to crystal radius a between zero and $a(0, t)$ (such as (3.4)–(3.7)), can be simplified further by changing the upper limit to infinity.

The existence of the quasi-steady solution, as described by (4.6), implies that a balance must exist between $(H-h)R_P$, the total rate of production of solid by crystallization, and R_S, the rate of sedimentation of crystals to form a cumulate pile. From (3.4), (3.5) and (4.6) we indeed see that

$$(H-h)R_P = R_S = 4\pi(H-h)^2 NV/\lambda, \tag{4.7}$$

in which N, V and λ are all functions of time, varying over the longer timescale t_c. The crystal production rate (and hence the rate of release of latent heat) is therefore proportional to the instantaneous nucleation and growth rates. The quasi-steady state described here may be viewed as an extension of the steady-state model proposed by Martin & Nokes (1989).

5. The simplified model in the quasi-steady limit

In order that we may isolate the essential dynamical balances for our model system, we shall now non-dimensionalize the model equations in the quasi-steady limit. First, we define dimensionless fluid, liquidus and roof temperatures θ, θ_L and θ_R by

$$\theta = \frac{T-T_{ref}}{\Delta T}; \quad \theta_L = \frac{T_L-T_{ref}}{\Delta T}; \quad \theta_R = \frac{T_R-T_{ref}}{\Delta T}, \tag{5.1}$$

where T_0 is the liquidus temperature T_L corresponding to the initial fluid composition C_0, as given by (2.8). T_{ref} is some reference temperature, which may be chosen to be the limiting temperature of the chamber as $t \to \infty$, and $\Delta T = (T_0 - T_{ref})$. For a fixed roof temperature T_R, the natural choice for T_{ref} would simply be $T_{ref} = T_R$.

The crystallization process is driven by the convective cooling of the fluid. The convective cooling timescale is (cf. (4.1))

$$t_{c0} = H\rho c_p \Delta T/\mathscr{F}_0, \tag{5.2}$$

where $\mathscr{F}_0 = \rho c_p J_0 \Delta T^{\frac{4}{3}}$ is a reference heat flux and J_0 is given by (2.4) with kinematic viscosity $\nu_0 = \nu(T_0)$. We define $\chi = \nu/\nu_0$ to be the dimensionless viscosity. From (5.2), we also define a dimensionless time

$$\tau = t/t_{c0}, \tag{5.3}$$

and rescale the depth of the crystal cumulate with respect to H, so that $d = h/H$ is the dimensionless cumulate thickness.

Finally, we rescale the growth and nucleation rates. In the present model, the only externally imposed temperature difference is ΔT, so we define the dimensionless growth and volumetric nucleation rates to be

$$v(\theta_L - \theta) = V/V_0 \quad \text{and} \quad \tilde{n}(\theta_L - \theta_R) = \tilde{N}/\tilde{N}_0, \tag{5.4}$$

where $V_0 = V(\Delta T)$ and $\tilde{N}_0 = \tilde{N}(\Delta T)$. From (2.5), the average nucleation rate N_0 (per unit chamber volume) has scale $N_0 = (h_{b0}/H)\tilde{N}_0$, where $h_{b0} = \rho c_p \kappa \Delta T/\mathscr{F}_0 \sim 6.4(\nu\kappa/g\alpha\Delta T)^{\frac{1}{3}}$ is the reference upper boundary-layer thickness. Therefore, the dimensionless nucleation rate n has the form

$$n(\theta_L - \theta_R) = N/N_0 = \chi^{\frac{1}{3}}(\theta - \theta_R)^{-\frac{1}{3}}(1-d)^{-1}\tilde{n}(\theta_L - \theta_R). \tag{5.5}$$

5.1. *Parametric forms for the crystal nucleation and growth rates*

We choose the following simple parametric forms for the dimensionless volumetric nucleation and growth rates, $\tilde{n}$ and v, as functions of the undercooling in the cold upper thermal boundary layer ($u = \theta_L - \theta_R$), and in the convecting bulk fluid ($u = \theta_L - \theta$) respectively:

$$\tilde{n}(u) = \begin{cases} 0 & \text{if } u \leqslant \epsilon \\ ((u-\epsilon)/(1-\epsilon))^p & \text{if } u > \epsilon \end{cases} \quad \text{and} \quad v(u) = u^q. \tag{5.6}$$

At zero undercooling ($u = 0$), both nucleation and growth rates are zero, whilst at $u = 1$, which corresponds to a dimensional undercooling ΔT, both $\tilde{n}$ and v are unity, as required by the scaling (5.4). The constant ϵ is the dimensionless nucleation delay, and represents the minimum undercooling required for crystal nucleation to occur (Dowty 1980), scaled by the reference temperature scale ΔT. The exponents p and q are both positive, and typically exceed unity for magmatic fluids (Kirkpatrick 1977; Brandeis & Jaupart 1986).

The parametric form (5.6) cannot be used to describe fluids for which the growth and nucleation rates do not increase monotonically with u for the applicable range of undercooling, although it would be a simple matter to extend the current investigation to such fluids. Note also that the qualitative behaviour described below when the nucleation function is linear ($p = 1$), and has non-zero nucleation delay ($\epsilon > 0$), is similar to that predicted for highly nonlinear nucleation functions ($p \gg 1$), but with zero nucleation delay ($\epsilon = 0$).

5.2. *The coupled model for cooling and crystallization*

Upon rescaling variables as described above, the model equations (2.1), (2.9) and (2.2) reduce to the following dimensionless equations for the conservation of heat, mass and cumulate-layer thickness in the quasi-steady limit:

$$(1-d)\dot{\theta} = -f + AS(1-d)r_p; \tag{5.7}$$

$$\dot{\theta}_L = -A(1-k_D)(\theta_\alpha - \theta_L)r_p; \tag{5.8}$$

$$\dot{d} = A(1-d)r_p, \tag{5.9}$$

where the dots denote differentiation with respect to τ and the Stefan number $S = \mathscr{L}/c_p\Delta T$. The dimensionless heat flux, f, and crystal production (sedimentation) rate, r_p, are given by

$$f = \mathscr{F}/\mathscr{F}_0 = \chi^{-\frac{1}{3}}(\theta - \theta_R)^{\frac{4}{3}}; \tag{5.10}$$

$$r_p = R_P/R_{P0} = \chi(1-d)nv, \tag{5.11}$$

in which $R_{P0} = 4\pi H N_0 V_0/\lambda_0$ and $\lambda_0 = 2g'/9\nu_0$. The dimensionless parameter A is defined by

$$A = 4\pi H N_0 V_0 t_{c0}/\lambda_0, \tag{5.12}$$

and is a measure of the amount of solid which would be produced if the constitutional undercooling were maintained equal everywhere to the initial imposed temperature difference ΔT throughout the cooling history of the fluid. The value $A = 1$ corresponds to the case in which the entire chamber would become solid over the timescale t_{c0}. In the following sections, we shall concentrate on the asymptotic limit $A \gg 1$, in which crystals would grow very rapidly if undercooled by ΔT. We shall see in the following sections that, in this limit, the release of latent heat during crystallization serves to limit significantly the rate of crystallization as the fluid cools.

Note that by eliminating r_p from (5.8) and (5.9), and integrating the result we may obtain the simple expression,

$$d = 1 - \left(\frac{\theta_\alpha - 1}{\theta_\alpha - \theta_L}\right)^{1/(1-k_D)}, \tag{5.13}$$

which relates the liquidus temperature θ_L (and hence the fluid composition) to the depth d of the crystal cumulate. This relationship follows from the observation that, in the quasi-steady limit, the nucleation, growth and settling mechanism described in this paper is an example of perfect fractionation, with newly formed crystals effectively being removed immediately from the convecting bulk (equation (4.7)).

5.3. *Initial conditions*

While the convecting bulk fluid is still superheated ($T > T_L$), any crystals nucleated in the upper boundary layer will melt upon extraction from the boundary layer. Hence, we may neglect this initial transient and commence calculation once the melt superheat has been removed. Thus, the dimensionless initial conditions ($\tau = 0$) for (5.7)–(5.9) are $\theta = \theta_L = 1$ and $d = 0$.

To complete the mathematical formulation, we must describe the evolution of the roof temperature θ_R. In §7, we consider two simple examples which have been chosen to illustrate the influence of the roof conditions upon the evolution of the melt, namely a fixed roof temperature and a prescribed, varying roof heat flux. However, before launching into this discussion, we shall first outline in §6 the general behaviour of the model system in the limit $A \gg 1$. Conditions for which $A \gg 1$ are described in Appendix D.

6. The limit $A \gg 1$: growth- and nucleation-limited crystallization

As heat is removed through the roof of the chamber, the mean fluid temperature θ must decrease. Therefore, from (5.7) it follows that the convective heat flux, f, always exceeds the rate of release of the latent heat of solidification, $AS(1-d)r_p$. Combining this constraint with the expression for the dimensionless crystal production rate r_p, yields the condition

$$AS(1-d)^2 \chi n v \lesssim f. \tag{6.1}$$

Typically $S, f, (1-d) \sim O(1)$ and $\chi \geqslant 1$. Therefore, in the limit $A \gg 1$, the product

$$nv \lesssim A^{-1} \ll 1. \tag{6.2}$$

Using the model nucleation and growth laws (5.6) for n and v, it follows that there are two different regimes under which the constraint (6.2) may be satisfied. Either the

crystal nucleation rate is very small ($n \sim A^{-1}$), or the crystal growth rate is very small ($v \sim A^{-1}$). Each of these regimes may occur during the cooling of a single fluid body.

6.1. *The growth-limited regime*

If the undercooling in the thermal boundary layer, $(\theta_L - \theta_R)$, exceeds the nucleation delay, ϵ, then nucleation and growth of crystals occurs immediately after the bulk convecting fluid is cooled to the liquidus temperature. As we argued above, any crystals nucleated before this time are remelted upon entering the superheated interior. Therefore, if $(T_L - T_R) > \epsilon$, then the condition (6.2) requires that the dimensionless growth rate $v \sim O(A^{-1})$. For the parametric form (5.6) for v, this corresponds to an undercooling

$$\theta - \theta_L \sim O(A^{-1/q}) \ll 1. \tag{6.3}$$

We term this the *growth-limited regime*, because the undercooling of the bulk fluid remains very small and the crystal growth is suppressed. The approach to this regime is rapid: by combining (5.11), (5.7) and (5.8), we see that the time evolution of the melt undercooling is given by

$$\dot{\theta}_L - \dot{\theta} = \frac{f}{1-d} - A[S + (1-k_D)(\theta_\alpha - \theta_L)]\,\chi(1-d)\,n(\theta_L - \theta_R)\,v(\theta_L - \theta). \tag{6.4}$$

At early times, $n(\theta_L - \theta_R) \sim 1$, and thus for a growth rate function of form (5.6), the crystal production rate becomes slaved to the extracted heat flux over the dimensionless timescale $A^{-1/q} \ll 1$. Equation (6.4) illustrates the fundamental controls upon crystallization which apply during the growth-limited regime, through the factor $[S + (1-k_D)(\theta_\alpha - \theta_L)]$. Crystallization cannot proceed too rapidly because (i) the latent heat of crystallization must be extracted from the chamber to prevent raising the fluid temperature, and (ii) rapid crystallization depresses the liquidus temperature by altering the fluid composition, thereby acting to decrease the undercooling which drives crystal growth.

By substituting $\theta \sim \theta_L$ into the evolution equations (5.7) and (5.8) and solving for r_p, we also see that, in the limit $A \gg 1$, the dimensionless volumetric crystal production rate is, to leading order,

$$r_p = \frac{f}{A(1-d)}[S + (1-k_D)(\theta_\alpha - \theta_L)]^{-1}, \tag{6.5}$$

which demonstrates again the control of latent heat release and liquidus slope upon the rate of crystallization. If we substitute (6.5) into the heat balance (5.7), we find that the rate of cooling of the fluid is reduced by the factor $[1 + S/(1-k_D)(\theta_\alpha - \theta_L)]$, which may be interpreted as an effective increase in the specific heat of the crystallizing system.

The growth-limited regime continues so long as there is substantial nucleation within the upper boundary layer ($n \sim O(1)$), i.e. while $(\theta_L - \theta_R) \gtrsim O(\epsilon)$. However, if the boundary-layer undercooling approaches the nucleation delay ϵ, nucleation of new crystals must decrease, and the *nucleation-limited regime* described below commences. In the limit $A \gg 1$, the thickness of cumulate associated with the growth-limited regime may be found (approximately) by setting the liquidus temperature $\theta_L = \theta_R + \epsilon$ in (5.13).

6.2. *The nucleation-limited regime*

When the liquidus temperature falls close to the value $\theta_R + \epsilon$, the rate of nucleation of crystals decreases rapidly and a new balance is reached, in which the roof undercooling, $(\theta_L - \theta_R)$, remains close to the critical nucleation delay ϵ. In this regime, the interior

undercooling, $(\theta_L-\theta)$, may increase and crystal growth is no longer suppressed. However, the fluid temperature, θ, remains above the roof temperature, θ_R, and hence the interior undercooling is still insufficient for interior nucleation. The constraint (6.2) is now satisfied by the dramatic reduction in the nucleation rate within the thermal boundary layer, with

$$n(\theta_L-\theta_R) \lesssim O(A^{-1}) \ll 1. \tag{6.6}$$

The boundary layer undercooling $(\theta_L-\theta_R)$ can only evolve by an amount $O(A^{-1/p})$ as the fluid continues to cool, and so, to leading order, the liquidus temperature follows the temperature of the roof $(\theta_L \sim \theta_R+\epsilon)$. Hence, to leading order, the rate of crystal production in the nucleation-limited regime is, from (5.8),

$$r_p = -\frac{\dot{\theta}_R}{A(1-k_D)(\theta_\alpha-\theta_R-\epsilon)}, \tag{6.7}$$

which suggests that during the nucleation-limited regime crystallization is now controlled by the evolution of the roof temperature, θ_R. If the roof temperature is maintained at a constant value, (6.7) implies that there is no further crystallization once the nucleation-limited regime is reached. The undercooling in the thermal boundary layer is insufficient for effective nucleation, and the interior undercooling increases towards the nucleation delay, ϵ. The final state is a metastable state, in which the fluid is everywhere supercooled to the nucleation delay, ϵ, but no crystallization occurs.

However, if the roof temperature is allowed to vary – or, more specifically, to decrease – there is still significant crystallization associated with the nucleation-limited regime. The crystal production rate given by (6.7) is such that the liquidus temperature decreases at the same rate as the roof temperature, so that the undercooling, $(\theta_L-\theta_R)$, within the upper thermal boundary layer remains approximately equal to ϵ. If the crystal production rate were larger than that given by (6.7), the liquidus temperature would decrease more rapidly than the roof temperature and the boundary layer cease to be undercooled sufficiently for nucleation to continue. Conversely, if r_p were to decrease slightly, then $(\theta_L-\theta_R)$ would increase and crystal production accelerate. The control exercised by the evolution of the roof during the nucleation-limited regime suggests that an accurate roof model is required for the study of a given physical situation.

6.3. *Size grading in the crystal cumulate*

As the crystal cumulate is deposited, the mean size of the crystals sedimented varies with depth. This reflects the varying fluid conditions through the crystallization history. By evaluating (3.7) in dimensionless form, we obtain

$$\bar{a}_d = \Gamma(\tfrac{4}{3})(3HV_0/\lambda_0)^{\frac{1}{3}}[\chi(1-d)v]^{\frac{1}{3}}. \tag{6.8}$$

Hence, there is an increase in mean crystal radius $\bar{a}_d$ if the fluid viscosity χ or the crystal growth rate v increase, but a decrease in $\bar{a}_d$ associated with the increased efficiency of sedimentation as the fluid depth $(1-d)$ decreases. During the growth-limited regime, the growth rate v is given to leading order from (6.4) as

$$v = (f/n)(A(1-d)^2\chi[S+(1-k_D)(\theta_\alpha-\theta_L)])^{-1}, \tag{6.9}$$

where $\theta \sim \theta_L$. Therefore, from the definition (5.10) for the dimensionless heat flux f, and (5.6) for the volumetric nucleation rate $\tilde{n}$, we see that during the growth-limited regime,

$$v \propto A^{-1}\chi^{-\frac{5}{3}}(\theta-\theta_R)^{\frac{5}{3}}(\theta_L-\theta_R-\epsilon)^{-p}. \tag{6.10}$$

As the fluid cools, the dimensionless viscosity χ increases (or stays constant), while the undercooling $(\theta_L - \theta_R)$ in the thermal boundary layer decreases. If the fluid viscosity remains constant, then (6.10) implies that the cumulate should be *normally graded* (small crystals over large) if the nucleation law is locally weakly nonlinear ($p < \frac{5}{3}$), but *inversely graded* (large crystals over small) if the nucleation law is locally strongly nonlinear ($p > \frac{5}{3}$), or if the boundary-layer undercooling approaches the nucleation delay ϵ. If the fluid viscosity increases with decreasing temperature, the normal grading is strengthened. Note that in the growth-limited regime, the crystals deposited are relatively small ($\bar{a}_d \propto A^{-\frac{1}{3}}$). The tendency for normal grading is a reflection of the gradual decrease in the cooling rate. This increases the growth time of the crystals relative to their sedimentation time, and as a result, the mean size of crystals which sediment to the base of the melt becomes progressively smaller.

In the nucleation-limited regime, much larger growth rates are possible because the constraint (6.2) is now satisfied by having $n \sim O(A^{-1})$. As the fluid continues to cool, the temperature difference, $(\theta - \theta_R)$, between the bulk convecting fluid and the roof continues to decrease towards zero, while the boundary-layer undercooling $(\theta_L - \theta_R)$ remains approximately equal to ϵ. Therefore, the constitutional undercooling in the bulk fluid, $(\theta_L - \theta)$, can increase from $O(A^{-1/q})$ to $O(1)$ during the nucleation-limited regime. This corresponds to a steady increase in the growth rate v, and hence from (6.8) we find that the crystal cumulate is typically inversely graded during the nucleation-limited regime. Furthermore, owing to the more rapid growth rates, crystals sedimented during this latter period are typically larger than those which settled during the earlier growth-limited regime by a factor of $O(A^{\frac{1}{3}}) \gg 1$. However, in some cases (see §7.2 below), during the nucleation-limited regime, the crystal growth rate varies only slowly; in such cases, the evolution of the mean crystal radius is determined by the evolution of the fluid viscosity, χ, and the thickness, $(1-d)$, of the convecting region. In cases in which the viscosity variation is weak, the reduction in settling time as the thickness of the convecting region decreases results in the cumulate becoming normally graded.

7. The limit $A \gg 1$: sample solutions

We shall now illustrate the results of the asymptotic analysis for the limit $A \gg 1$, presented in §6, by reference to two specific examples. Each exhibits one or both of the nucleation- and growth-limited regimes, but the overall dynamics differ markedly between them. Parameters common to all calculations are $A = 10^3$; $S = 1$; $k_D = 0$; and $\theta_\alpha = 2$. For simplicity, the nucleation and growth laws are linear ($p = q = 1$), and except where stated to the contrary, the fluid viscosity is constant.

7.1. *Fixed roof temperature: cooling above the eutectic*

The simplest case is a fixed roof temperature above the eutectic (see figure 3), for which a final equilibrium may be reached in which the original fluid body is part solid and part liquid. Solutions obtained from the asymptotic expressions (6.5) and (6.7) for the crystal production rate, r_p, are indistinguishable from the calculations.

At early times, crystallization is growth-limited, with the overall rate of crystal production limited by the concomitant lowering of the liquidus temperature, and by the release of latent heat. For $A = 10^3 \gg 1$, the curves for the fluid temperature θ and the liquidus temperature θ_L are indistinguishable during this initial phase. At $\tau \sim 3.6$, the undercooling $(\theta_L - \theta_R)$ in the cold upper boundary layer approaches the nucleation delay $\epsilon = 0.1$, which leads to a reduction in the rate of crystal nucleation. This event

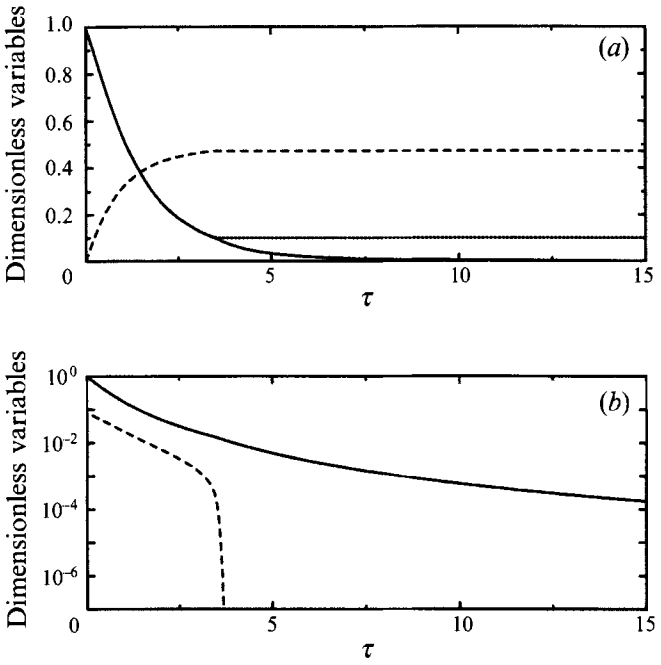

FIGURE 3. Numerical calculation to illustrate the evolution of the model system when the upper boundary is suddenly lowered to a fixed temperature ($\theta_R = 0$) above the eutectic. The nucleation and growth laws are linear, with dimensionless nucleation delay $\epsilon = 0.1$, and the fluid viscosity is constant. Other parameters are given in the text. In (*a*), the bulk fluid temperature θ (——), liquidus temperature θ_L (·····) and the cumulate thickness d (– – –) are plotted, and in (*b*), the relative Rayleigh number Ra/Ra_0 (——) and relative crystal volume fraction Φ/Φ_0 (----) are presented as functions of time τ.

is marked by a sharp transition. There then follows the second, nucleation-limited, regime in which the interior undercooling, $(\theta_L - \theta)$, gradually increases, while the liquidus temperature remains at $\theta_L = \theta_R + \epsilon$ and there is negligible further crystallization. At the transition between the growth- and nucleation-limited regimes, the crystal volume fraction Φ also falls rapidly towards zero. The final state is one in which the alloy is not completely solidified, but rather in a metastable equilibrium. Although the fluid is supercooled, further crystallization is no longer possible in our model system because the constitutional undercooling is nowhere sufficient for nucleation to occur, and all free crystals have settled out of the bulk interior. In practice, one might expect crystallization to continue by growth of crystals in the cumulate pile.

Throughout crystallization, the Rayleigh number decreases as the driving temperature difference $(\theta - \theta_R)$ and the fluid depth $(1-d)$ are lowered. After the dimensionless calculation time $\tau = 50$, the Rayleigh number has fallen by four orders of magnitude. The numerical calculations of Hansen *et al.* (1992) for infinite-Prandtl-number convection in a fluid body with small aspect ratio suggest that when the Rayleigh number falls below about 10^7, the system may no longer be considered to be well-mixed. The precise moment at which this occurs in our model depends upon the initial Rayleigh number Ra_0. For the present calculation, the convecting fluid may be considered well-mixed at least until $\tau = 50$ if the initial Rayleigh number $Ra_0 \gtrsim 10^{11}$.

In figure 4, we have plotted the mean crystal radius $\bar{a}_d$ as a function of depth d in the cumulate pile, as measured from the floor of the chamber. For illustration, to

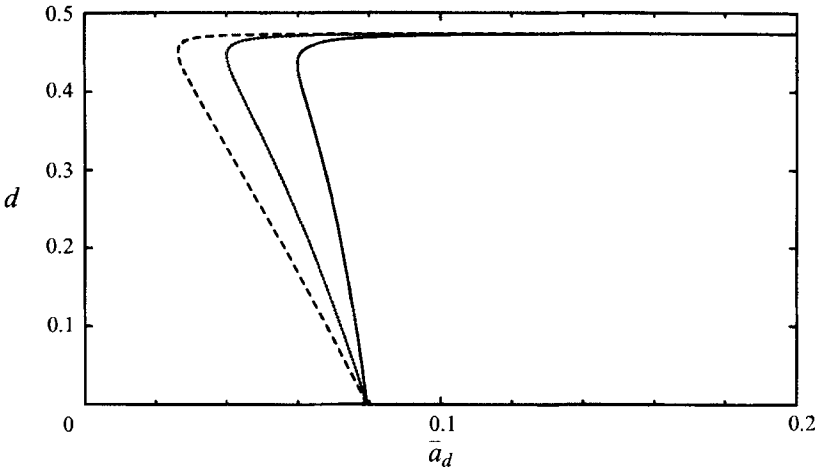

FIGURE 4. Size grading in the cumulate pile for a fixed roof temperature above the eutectic. The effect of variable viscosity is investigated using the arbitrary law $\chi \equiv \nu/\nu_0 = r^{(1-\theta)}$ (——, $r = 1$; ·····, $r = 10$; – – –, $r = 100$). In each case, there is a weak normal grading associated with the growth-limited regime, followed by a stronger inverse grading in the nucleation-limited regime. The increase in viscosity as the magma cools leads to a strengthening of the normal grading. For a basaltic magma (see table 1), unit dimensionless mean crystal radius $\bar{a}_d$ corresponds to crystals of radius between 0.1 mm and 10 cm.

investigate the effects of weakly variable viscosity, we have repeated the calculation using a simple model viscosity law $\chi = r^{(1-\theta)}$, with $r = 10$ and 100. This corresponds to exponential viscosity increases by factors of 10 and 100 respectively as the fluid cools from $\theta = 1$ to $\theta = 0$. Larger viscosity variations would result in a stagnant viscous lid forming over the convective part of the fluid (Davaille & Jaupart 1993), for which a constant roof temperature would no longer be appropriate. The cumulate is characterized by a moderate normal grading (small crystals over large) during the growth-limited regime. This grading is more marked in fluids whose viscosity increases rapidly with cooling, as suggested by (6.10). Towards the top of the cumulate pile ($d \sim 0.5$), the grading reverses as nucleation-limited dynamics take over, and a thin layer of inversely graded cumulate develops. The larger crystal radii are associated with an increase in the undercooling $(\theta_L - \theta)$ of the bulk convecting fluid.

7.2. *Variable roof temperature*

We now analyse the crystallization associated with a simple prescribed model for the dimensionless heat flux, namely

$$f(\tau) = 0.2(1 + \tau/0.4)^{-\frac{3}{4}}. \tag{7.1}$$

The critical aspect of (7.1) is that the roof temperature is allowed to decrease with the fluid temperature, through (5.10) for f. In this sense, we mimic the manner in which the contact temperature might decrease if cooling were partially controlled by heat transfer through some overlying solid or viscous fluid lid. Our sole aim is to exhibit the new qualitative behaviour with a decreasing roof temperature. For example, similar solutions occur when a fixed flux, $f = \text{const.}$, is applied.

If the nucleation delay is relatively small ($\epsilon = 0.1$), nucleation commences immediately in the cold upper boundary layer (figure 5) and the rate of growth of crystals is limited by the overall heat balance. However, at $\tau \sim 0.5$, the boundary-layer

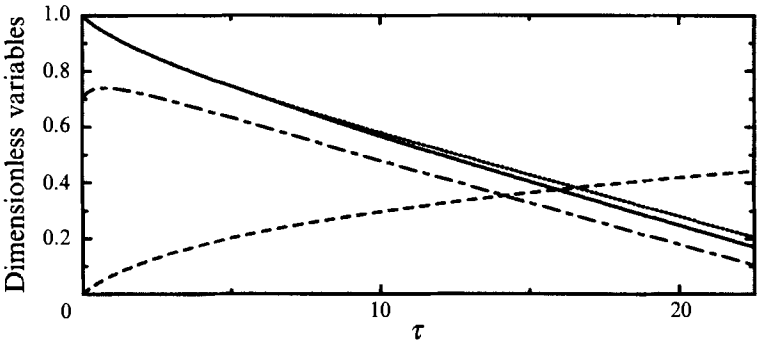

FIGURE 5. Numerical calculation for specified decaying roof flux $f = 0.2(1+\tau/0.4)^{-\frac{3}{4}}$, nucleation delay $\epsilon = 0.1$ and eutectic temperature $\theta_E = 0.2$. Legend as for figure 3, with roof temperature θ_R (– · – · –).

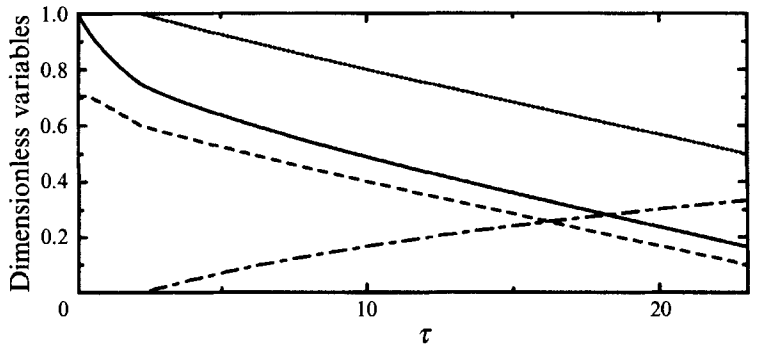

FIGURE 6. Same as figure 5, with the same decaying roof flux f, but larger nucleation delay ($\epsilon = 0.4$) and dimensionless eutectic temperature $\theta_E = 0.5$. Legend as for figure 5.

undercooling approaches the nucleation delay and the growth-limited regime is succeeded by the nucleation-limited regime. In contrast to the previous examples (figure 3), the transition between regimes is gradual. Thereafter, the fluid temperature, θ, continues to decrease, as does the roof temperature, such that the undercooling within the thermal boundary layer, $(T_L - T_R)$, remains equal to the nucleation delay, ϵ. This reduction in the roof temperature allows the liquidus temperature to decrease and so crystal production continues. Hence, there is a finite cumulate thickness associated with the nucleation-limited regime, again in contrast to the case of a fixed roof temperature (see figure 3). We halt the calculation when the bulk liquidus temperature reaches the eutectic, as we do not model the settling of the second crystalline phase.

When the nucleation delay is larger ($\epsilon = 0.4$, see figure 6), the initial undercooling in the boundary layer is now insufficient for crystal nucleation to occur immediately. Therefore, the bulk fluid temperature, θ, decreases relatively rapidly, as there is no latent heat being released, and the roof temperature, θ_R, decreases rapidly in response. However, by the dimensionless time $\tau \sim 2.3$, the boundary-layer undercooling, $(\theta_L - \theta_R)$, has fallen sufficiently to allow nucleation to commence. The system immediately enters the nucleation-limited regime, with a large undercooling in the fluid interior, although the interior undercooling remains smaller than the nucleation delay. In this second example, there is no initial growth-limited regime, and we term this regime *delayed nucleation*. The subsequent evolution is similar to the example in figure 5.

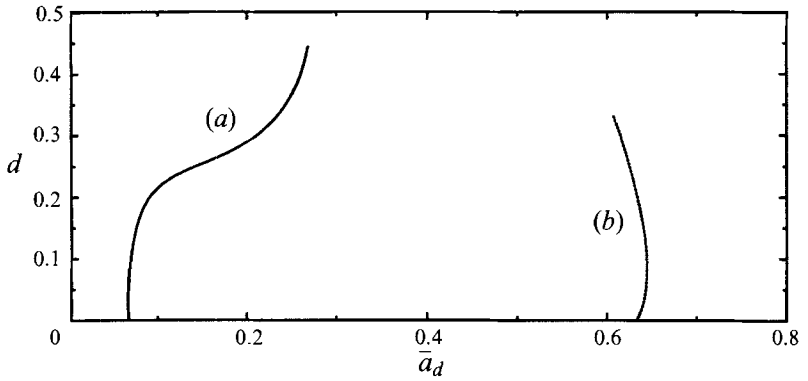

FIGURE 7. Size grading in the cumulate pile for variable roof flux. The two curves drawn correspond to the calculations presented in (*a*) figure 5 (——), and (*b*) figure 6 (·····). For the smaller nucleation delay, there is a normal grading associated with the growth-limited regime, followed by an inverse grading during the nucleation-limited regime. For the larger nucleation delay, there is no growth-limited regime. The crystal pile is normally graded, and the exception of a thin, inversely graded, basal layer. The larger crystal sizes in (*b*), compared with (*a*), are associated with a greater undercooling in the convecting interior.

Finally, in figure 7, we plot the crystal grading in the cumulate pile for these last two examples. For the case in which there is immediate nucleation (figure 7*a*), the grading is first weakly normal, followed by a stronger inverse grading. The reversal of the crystal grading is associated with the change from the growth-limited regime to the nucleation-limited regime, during which the growth rate of crystals, and hence their mean size, increases. For the nucleation-delayed case (figure 7*b*), the crystal pile is inversely graded throughout.

8. Discussion

We have presented a new theory of the nucleation, growth and sedimentation of a dilute suspension of crystals from a turbulently convecting fluid cooled from above. We have described how a quasi-steady crystal distribution becomes established when the typical residence time of crystals in the convecting interior is much less than the convective cooling time. In this quasi-steady limit, the rate of solidification of crystals within the convecting bulk fluid is balanced by the rate of sedimentation at the floor. This leads to a simple and tractable model of the thermal evolution of the chamber. By coupling a description of the cooling of a turbulently convecting fluid cooled from above with some model crystal nucleation and growth laws, we have calculated how the thickness of the sediment layer and the mean grain size of the sediment layer vary with time. The model applies whenever the crystal fraction is small.

The thermodynamic controls upon the rate of crystallization are determined by a dimensionless parameter A, which compares the convective cooling time with the time for solidification if the fluid undercooling were everywhere equal to the initial imposed temperature difference between the roof and the fluid. The control is strongest when A is large. Our model suggests that for a fixed roof temperature, the crystal production is rate-limited by the growth kinetics in the first instance, and the fluid temperature is maintained just below the liquidus. However, as the fluid continues to cool, the undercooling in the cold upper boundary layer falls close to the critical value required to nucleate crystals. At this stage, the rate of nucleation of new crystals diminishes dramatically, the fluid becomes more undercooled, and crystal production is rate-

limited by the nucleation kinetics. We have also demonstrated that when the flux extracted through the roof is insufficient for immediate nucleation of crystals, crystallization is delayed until the undercooling in the thermal boundary layer reaches the critical nucleation delay. Only then many nucleation-limited crystallization commence.

In all cases, we have determined the size-grading within the crystal cumulate which forms at the floor. This grading reflects the undercooling in the fluid at the time of sedimentation, and can be either normal or inverse. Typically, the growth-limited regime is associated with normal grading for weakly nonlinear crystal growth laws. In contrast, sediment formed during the nucleation-limited regime may exhibit normal or inverse grading, depending upon the roof conditions. During the cooling of a single fluid body, both styles of grading may be observed. Here, we have only considered the crystallization of a single mineral phase, and hence our predictions apply only to the lower part of a fully solidified fluid body.

The model presented in this paper is, as far as we know, the first attempt at determining how vigorous thermal convection may interact with the formation and suspension of dense crystals within the convecting part of the fluid. This interaction controls the overall cooling history of the fluid body and the structure of the final solidified product. However, immediate application of our present theory to magmatic bodies is not straightforward. The dimensional analyses presented in Appendices A and B suggest that the circumstances in which crystals are extracted from the upper boundary layer with negligible radius, and in which there is a dilute crystal suspension, a short crystal residence time and strong thermodynamic control ($A \gg 1$), arise only for relatively inviscid basaltic magmas. In addition, we require a relatively low nucleation rate and a relatively high crystal growth rate, conditions which are best met when the temperature difference driving convection is close to the nucleation delay. Nevertheless, we do not expect relaxation of most of these assumptions to make a significant difference to the main qualitative results of our study, with the important exception of the dilute-suspension assumption ($\Phi \ll 1$). The experiments of Sparks *et al.* (1993) and the numerical calculations of Rudman (1992) clearly demonstrate marked changes in sedimentation behaviour once the volume fraction of suspended particles is sufficiently large for the convection itself to be adversely affected.

In studying the crystallization of silicate fluids, such as basaltic magmas, we must also consider the effects of strongly variable viscosity. Our calculations described in §7.1 suggest that the normal crystal grading associated with the growth-limited regime strengthens when the fluid viscosity decreases. However, two important effects were not included. First, we did not explicitly treat the stagnant viscous layer which should form near the roof when there is a large viscosity difference between the fluid at the cold wall and the bulk convecting fluid (Richter 1978; Davaille & Jaupart 1993), and second, we neglected the effect of fluid viscosity upon the crystal nucleation and growth laws. Nevertheless, we expect the most important effect of increasing viscosity to be the reduction in the efficiency of crystal settling, thereby increasing the volume fraction of crystals suspended in the convecting fluid. A further consideration for deep magmatic bodies is the effect of hydrostatic pressure upon the liquidus relationship, which may lead to substantial basal crystallization (see Solomatov & Stevenson 1993*a*, *b* for a discussion of how this might relate to crystal settling in magma oceans). In this paper, we have ignored all crystallization with the exception of the growth of free crystals nucleated near the roof.

The work presented here began while the authors were participants in the 1992

Geophysical Fluid Dynamics Summer Program at Woods Hole Oceanographic Institution. R.A.J. was supported by a UCAR Fellowship in Ocean Modelling. We have benefited from discussions with Anne Davaille, Mark Davis, Phil Ihinger, Claude Jaupart, David Pyle, Don Snyder and Steve Tait, and the final manuscript has been greatly improved by comments from the referees.

Appendix A. Extraction of crystals from the upper boundary layer

In this paper, we have assumed that crystal growth occurs predominantly within the bulk convecting interior, rather than in the cold upper boundary layer, where crystals nucleate. This requires rapid extraction of crystals from the thermal boundary layer, either by gravitational settling, or by advection in the cold downgoing plumes which result from instability of the upper boundary. In this Appendix, we shall first determine when rapid extraction occurs for a vigorously convecting fluid, and then discuss how the precise style of crystal extraction may differ between particular fluids.

Consider a spherical crystal nucleated at time $t = 0$ within the cold upper boundary layer. After time t, the crystal has radius $a = V_b t$, where V_b is the crystal growth rate within the boundary layer. If the crystal falls at its Stokes settling speed $W_S(a) = 2g'a^2/9\nu$, then it settles out of a boundary layer of thickness h_b in time

$$t_{settle} \sim [27\nu_b h_b/(2g' V_b^2)]^{\frac{1}{3}}, \tag{A 1}$$

where ν_b is the kinematic viscosity within the boundary layer. The crystal has radius $a_b \sim V_b t_{settle}$ when it reaches the base of the thermal boundary layer. In deriving (A 1), we have assumed that crystals are nucleated with zero radius, although (A 1) remains correct to within $O(a_N/a_b)$ if crystals are nucleated with radius $a_N \ll a_b$. For crystals nucleated with non-zero radius, the settling timescale t_{settle} would be shorter than that given by (A 1).

The typical residence time for a crystal in the bulk convecting flow is $t_{res} \sim [(H-h)/\lambda V^2]^{\frac{1}{3}}$, where V is the crystal growth rate within the convecting bulk, and so

$$t_{settle}/t_{res} \sim [\nu_b h_b/(\nu H)]^{\frac{1}{3}} (V/V_b)^{\frac{2}{3}}, \tag{A 2}$$

where ν is the kinematic viscosity of the bulk convecting fluid. Note that even for fluids whose viscosity is strongly temperature-dependent, the viscosity variation ν_b/ν between the unstable thermal boundary layer and the convecting interior does not exceed an order of magnitude, since most of the temperature difference is contained within a stagnant viscous lid (Bruce 1989; Davaille & Jaupart 1993). Therefore, since $h_b/H \sim H \sim (\nu_b Ra_c/\nu Ra)^{\frac{1}{3}} \ll 1$ for a vigorously convecting flow (where $Ra_c \sim 10^3$), and typically $V < V_b$ because the constitutional undercooling is greatest within the thermal boundary layer, (A 2) implies that settling of crystals out of the cold upper boundary layer occurs over a shorter timescale than the residence time of a typical crystal in the convecting bulk. However, the rate of crystal growth within the boundary layer is higher than that in the interior. The fraction of the crystal growth which occurs within the thermal boundary layer is

$$a_b/\bar{a}_d \sim V_b t_{settle}/(V t_{res}) \sim [\nu_b h_b V_b/(\nu H V)]^{\frac{1}{3}}. \tag{A 3}$$

Therefore, if the dominant style of crystal extraction is gravitational settling, then crystals have negligible radius upon extraction from the boundary layer only for very vigorously convecting fluids in which $(Ra/Ra_c)^{\frac{1}{6}} \gg (\nu_b/\nu)^{\frac{4}{9}} (V_b/V)^{\frac{1}{3}}$.

For some fluids, extraction of crystals from the thermal boundary layer may occur more rapidly if the timescale for instability of the thermal boundary layer, t_{plume}, is

ρ	2.7×10^3	kg m^{-3}
$\Delta\rho$	10^2	kg m^{-3}
c_p	1.3×10^3	J kg^{-1} K^{-1}
κ	5.0×10^{-7}	m^2 s^{-1}
α	2.5×10^{-5}	K^{-1}
$\mathscr{L}$	5.0×10^5	J kg^{-1}
g	9.8	m s^{-2}
ΔT	10^{-1}–10^2	K
H	10^2–10^4	m
ν_0	10^{-2}–10	m^2 s^{-1}
$\tilde{N}_0$	10^0–10^6	#m^{-3} s^{-1}
V_0	10^{-10}–10^{-7}	m s^{-1}
Φ_0	10^{-5}–10^9	
A	10^{-4}–10^{14}	
$\Phi_0 A^{-\frac{1}{3}}$	10^{-3}–10^4	

TABLE 1. Physical parameters applicable to a cooling body of basaltic magma. Dimensional constants have been obtained from a number of sources, including Fenn (1977), Kirkpatrick (1977), Dowty (1980), Shaw (1972), Brandeis *et al.* (1984) and Brandeis & Jaupart (1986). The dimensionless groups Φ_0 and A are defined by (B 2) and (5.12) respectively. In addition, we give a range for $\Phi_0 A^{-\frac{1}{3}}$, which is the appropriate dimensionless group when determining the validity of the dilute and quasi-steady approximations.

much less than t_{settle}. In this case, crystals are advected out of the boundary layer by the cold downgoing plumes, rather than settling out gravitationally.

Instability of the thermal boundary layer occurs when the boundary layer has thickness (Howard 1964)

$$h_b \sim [\nu_b \kappa Ra_c/(g\alpha \Delta T)]^{\frac{1}{3}}. \tag{A 4}$$

The growth of the thermal boundary layer is diffusive, and hence is given by $h_b \sim (\kappa t)^{\frac{1}{2}}$. Therefore, the timescale for the release of cold plumes is

$$t_{plume} \sim (1/\kappa)[\nu_b \kappa Ra_c/(g\alpha \Delta T)]^{\frac{2}{3}}, \tag{A 5}$$

which, after some manipulation, implies that $t_{plume} < t_{settle}$ when

$$\nu_b \lesssim (g\kappa^2/V_b^3)[27\rho/(2\Delta\rho)]^{\frac{3}{2}}[\alpha \Delta T/(Ra_c)]^{\frac{5}{2}}. \tag{A 6}$$

For example, for a basaltic magma (see Table 1), with $V_b \sim 10^{-7}$ m s^{-1} and $\Delta T \sim 1$ K, crystal extraction from the thermal boundary layer occurs by plume detachment only when $\nu \lesssim 10$ m^2 s^{-1}. There is, however, a great deal of sensitivity to the chosen values of V_b and ΔT, and this constraint is relaxed significantly if the crystal growth rate is lower or the thermal forcing increased. Since the kinematic viscosity of a basaltic magma lies in the range 10^{-2}–10^1 m^2 s^{-1} (Shaw 1972) and $t_{plume}/t_{settle} \propto \nu_b^{\frac{2}{3}}$, it is likely that both crystal extraction mechanisms have a role to play, except for the most inviscid magmas.

We note that a similar analysis was performed by Sparks *et al.* (1993). By treating a crystal of constant size settling through the boundary layer, Sparks *et al.* (1993) concluded that gravitation settling is the dominant mechanism of crystal extraction for less viscous magmas, in marked contrast to the above result. The disagreement between these two studies arises from the differing treatments of the settling crystals. For a crystal of constant size, the settling time is proportional to $\nu_b^{\frac{4}{3}}$, while by combining (A 1) and (A 3), we see that, for a growing crystal, $t_{settle} \propto \nu_b^{\frac{4}{6}}$. The difference in exponents is sufficient to invert the result.

Appendix B. Validity of the passive-tracer assumption

In order that we may apply the experimental and theoretical results of Martin & Nokes (1988, 1989) for the settling of particles from a vigorously convecting fluid of constant viscosity, we must be able to treat the settling crystals as passive tracers away from the basal viscous boundary layers, which in turn requires that typical vertical velocities, W_{rms}, within the convecting bulk fluid exceed typical crystal settling velocities, $W_S(a)$. Following Kraichnan (1962) and Martin & Nokes (1989), mean turbulent velocities at mid-height of the chamber are given by

$$W_{rms} = \begin{cases} 0.06(\kappa/H)\,Ra^{\frac{2}{5}} & \text{if} \quad \delta_v < H/2; \\ 0.8(\kappa/H)\,Ra^{\frac{1}{3}}Nu^{\frac{1}{3}}Pr^{\frac{1}{3}} & \text{if} \quad \delta_v > H/2, \end{cases} \tag{B 1}$$

where $Pr = \nu/\kappa$ is the Prandtl number and Nu is the Nusselt number ($Nu \sim 0.16Ra^{\frac{1}{3}}$ for convection driven only from above). The viscous-boundary-layer thickness is $\delta_v \sim 3.2Pr^{\frac{1}{2}}H/Nu$ (Kraichnan 1962). Here, it is appropriate to seek a lower bound for W_{rms}. This is given by applying (B 1) for $\delta_v > H/2$ for all values of the viscous-boundary-layer thickness. By using the Stokes settling velocity $W_S(a)$, we then see that $W_S \ll W_{rms}$ for crystal radii a such that

$$a \ll \kappa^{\frac{1}{9}}g'^{-\frac{1}{2}}(g\alpha\,\Delta T)^{\frac{2}{9}}H^{\frac{1}{6}}\nu^{\frac{4}{9}}. \tag{B 2}$$

For the model presented here, in the quasi-steady state, the mean crystal radii are given by $\bar{a}_d \sim [(H-h)\,V/\lambda]^{\frac{1}{3}}$. Therefore, condition (B 2) corresponds to the constraint upon the crystal growth rate,

$$V \ll \kappa^{\frac{1}{3}}g'^{-\frac{1}{2}}(g\alpha\,\Delta T)^{\frac{2}{3}}H^{-\frac{1}{2}}\nu^{\frac{1}{3}}. \tag{B 3}$$

Using sample values from table 1 for basaltic magmas, with $\nu = 10^{-2}$ m^2 s^{-1}, $\Delta T = 1$ K and $H = 10^3$ m, (B 3) implies that the passive-tracer approximation is strictly valid only when $V \ll 10^{-7}$ m s^{-1} (cf. table 1). Note, however, that Martin & Nokes observed that the exponential law typically remains correct within 20% up to $W_S/W_{rms} \sim 0.5$, which allows us to relax the constraint (B 3) to a simple inequality.

The foregoing analysis is for crystals of mean radius. The ratio $W_S/W_{rms} \propto a^2$, and hence larger crystals might be expected to settle more rapidly than given by the exponential law of Martin & Nokes (1989) if (B 3) is only marginally satisfied for the mean crystal radius. This will lead to a skewing of the crystal size distribution, with fewer large crystals existing than is suggested by the general model solution (3.2) for the crystal size distribution.

Appendix C. Derivation of the boundary condition $\phi(0, t)$

To determine the boundary condition $\phi(0, t)$ for the crystal size distribution function, we first integrate (3.1) with respect to a from $a = 0$ to ∞ to obtain

$$\frac{\mathrm{d}}{\mathrm{d}t}\int_0^\infty \phi(a, t)\,\mathrm{d}a = V(t)\,\phi(0, t) - \frac{\lambda}{H-h}\int_0^\infty a^2\phi(a, t)\,\mathrm{d}a, \tag{C 1}$$

assuming that $\phi \to 0$ as $a \to \infty$. The left-hand side of (C 1) is the rate of change of the total number of crystals in suspension, per unit volume, while the second term on the right-hand side is the sedimentation rate. Hence, we may identify the first term on the right-hand side with the crystal nucleation rate $N(t)$, and the boundary condition for the crystal distribution function is

$$\phi(0, t) = N(t)/V(t). \tag{C 2}$$

Appendix D. Validity of the dilute and quasi-steady approximations

The model presented in this paper is valid only while the volume fraction of suspended crystals is small ($\Phi \ll 1$). In addition, the simplified model of §5 applies only when the typical crystal residence time within the convecting bulk is much shorter than the overall cooling timescale ($t_{res} \ll t_c$). In this Appendix, we shall describe the conditions under which these two approximations are valid, and determine when these conditions are met for magmatic fluids by using the values of physical constants listed in table 1.

In demonstrating the validity, or otherwise, of these two approximations, we start from the observation that during the initial transient, which comes immediately after commencement of crystal growth within the convecting bulk, the crystal fraction Φ increases monotonically, as does the bulk constitutional undercooling. This transient lasts only as long as the crystal residence time. If the dilute quasi-steady model presented in this paper predicts values of Φ and t_{res}/t_c which are both much less than unity, then the monotonicity of Φ during the transient ensures that the dilute approximation remains valid throughout the transient. Thereafter, so long as we continue to predict $\Phi \ll 1$ and $t_{res} \ll t_c$, the model continues to be correct by mathematical induction. However, if at any time either or both of these conditions are not met, then the model presented here ceases to be valid.

In practice, the two approximations are not entirely independent. The crystal fraction Φ in the quasi-steady limit is, upon evaluating the integral (3.6) in the quasi-steady limit,

$$\Phi = \Phi_0 n v^{\frac{1}{3}} \chi^{\frac{4}{3}} (1-d)^{\frac{4}{3}}, \tag{D 1}$$

where

$$\Phi_0 = (4\pi \Gamma(\tfrac{4}{3})/3^{\frac{2}{3}})(H^{\frac{4}{3}} N_0 V_0^{\frac{1}{3}}/\lambda_0^{\frac{4}{3}}). \tag{D 2}$$

Similarly, from (4.1) and (4.2) we can obtain the ratio of the crystal residence time to the overall cooling timescale,

$$t_{res}/t_c \sim (\Phi_0/A)\, v^{-\frac{2}{3}} (1-d)^{-\frac{2}{3}} (\theta - \theta_R)^{\frac{1}{3}}, \tag{D 3}$$

in which we have substituted for f and t_{c0} from (5.10) and (5.12) respectively. We may therefore determine the validity of the assumptions $\Phi \ll 1$ and $t_{res} \ll t$ from the values of Φ_0 and A, and from the evolution of n, v and χ during the growth- and nucleation-limited regimes. Except at the very late stages of crystallization, the fluid depth, $(1-d)$, and the driving temperature difference $(\theta - \theta_R)$, remain $O(1)$.

We may now determine under what conditions $\Phi \ll 1$ and $t_{res} \ll t_c$ for each of the growth- and nucleation-limited regimes. In the limit $A \gg 1$, this task is made easier by noting from the forms of (D 1) and (D 3) that if both approximations are valid for the growth-limited regime ($n \sim O(1)$, $v \sim O(A^{-1})$), then they must also be valid for the corresponding nucleation-limited regime ($n \sim O(A^{-1})$, $v \sim O(1)$). Hence we need only consider the growth-limited regime, for which we see from the constraint (6.1) that

$$\Phi \sim \Phi_0 A^{-\frac{1}{3}} n^{\frac{2}{3}} \chi^{\frac{8}{9}} (1-d)^{\frac{2}{3}} (\theta - \theta_R)^{\frac{4}{9}} S^{-\frac{1}{3}}; \tag{D 4}$$

$$t_{res}/t_c \sim \Phi_0 A^{-\frac{1}{3}} n^{\frac{2}{3}} \chi^{\frac{8}{9}} (1-d)^{\frac{2}{3}} (\theta - \theta_R)^{-\frac{5}{9}} S^{\frac{2}{3}}. \tag{D 5}$$

Therefore, if S, $(\theta - \theta_R) = O(1)$, the dilute and quasi-steady approximations are equivalent in the limit $A \gg 1$. We therefore require only that $A \gg 1$ and $\Phi_0 A^{-\frac{1}{3}} \ll 1$, noting that $A \propto \tilde{N}_0 V_0 \nu_0^{\frac{5}{3}} H (\Delta T)^{-\frac{2}{3}}$ and $\Phi_0 A^{-\frac{1}{3}} \propto \tilde{N}_0^{\frac{2}{3}} \nu_0^{\frac{10}{9}} (\Delta T)^{-\frac{1}{9}}$ (for basaltic magmas the constants of proportionality are 10^2 and 2×10^8 respectively).

By applying the physical values listed in table 1, we may now see that the model presented here can formally only be applied to relatively inviscid ($\nu_0 \lesssim 10^{-1}\ \mathrm{m^2\ s^{-1}}$),

relatively deep ($H \gtrsim 10^3$ m) magma bodies, in which the volumetric nucleation rate, $\tilde{N}_0$, is small and the crystal growth rate V_0 is large at undercooling equal to the applied temperature difference ΔT. These last two conditions are best met when the applied temperature difference is close to, or less than, the critical nucleation delay, i.e. the dimensionless nucleation delay ϵ is comparable to unity ($0.2 \lesssim \epsilon \lesssim 1$). Typical dimensional values for the nucleation delay are of the order 5–100 K, at which undercoolings crystal growth rates are indeed relatively large (Dowty 1980; Brandeis & Jaupart 1986).

REFERENCES

BARTLETT, R. W. 1969 Magma convection, temperature distribution and differentiation. *Am. J. Sci.* **269**, 169–182.

BOWEN, N. L. 1915 Crystal differentiation in silicate liquids. *Am. J. Sci.* **39**, 175–191.

BRANDEIS, G. & JAUPART, C. 1986 On the interaction between convection and crystallization in cooling magma chambers. *Earth Planet. Sci. Lett.* **77**, 345–361.

BRANDEIS, G. & JAUPART, C. 1987 The kinetics of nucleation and crystal growth and scaling laws for magmatic crystallization. *Contrib. Min. Petrol.* **96**, 24–34.

BRANDEIS, G., JAUPART, C. & ALLÈGRE, C. J. 1984 Nucleation, crystal growth and the thermal regime of cooling magmas. *J. Geophys. Res.* **89**, 10161–10177.

BRUCE, P. M. 1989 Thermal convection within the Earth's crust. PhD thesis, University of Cambridge.

CAMPBELL, I. H. 1978 Some problems with the cumulus theory. *Lithos* **11**, 311–323.

DAVAILLE, A. & JAUPART, C. 1993 Transient high-Rayleigh-number thermal convection with large viscosity variations. *J. Fluid Mech.* **253**, 141–166.

DOWTY, E. 1980 Crystal growth and nucleation theory and the numerical simulation of igneous crystallization. In *Physics of Magmatic Processes* (ed. R. Hargraves), pp. 419–485. Princeton.

FENN, P. M. 1977 The nucleation and growth of alkali fieldspars from hydrous melts. *Can. Mineral.* **15**, 135–161.

HANSEN, U., YUEN, D. A. & KROENING, S. E. 1992 Mass and heat transport in strongly time-dependent thermal convection at infinite Prandtl number. *Geophys. Astrophys. Fluid Dyn.* **63**, 67–89.

HORT, M. & SPOHN, T. 1991 Crystallization calculations for a binary melt cooling at constant rates of heat removal: implications for the crystallization of magma bodies. *Earth Planet. Sci. Lett.* **107**, 463–474.

HOWARD, L. N. 1964 Convection at high Rayleigh number. In *Proc. 11th Intl Congr. of Applied Mechanics, Munich 1964* (ed. H. Görtler), pp. 1109–1115. Springer.

HUPPERT, H. E. 1990 The fluid dynamics of solidification. *J. Fluid Mech.* **212**, 209–240.

JAUPART, C. & PARSONS, B. 1985 Convective instabilities in a variable viscosity fluid cooled from above. *Phys. Earth Planet. Inter.* **39**, 14–32.

KATSAROS, K. B., LIU, W. T., BUSINGER, J. A. & TILLMAN, J. E. 1977 Heat transport and thermal structure in the interfacial boundary layer in an open tank of water in turbulent free convection. *J. Fluid Mech.* **83**, 331–348.

KERR, R. C., WOODS, A. W., WORSTER, M. G. & HUPPERT, H. E. 1990 Solidification of an alloy cooled from above. Part 2. Non-equilibrium interfacial kinetics. *J. Fluid Mech.* **217**, 331–348.

KIRKPATRICK, R. J. 1976 Towards a kinetic model for the crystallization of magma bodies. *J. Geophys. Res.* **81**, 2565–2571.

KIRKPATRICK, R. J. 1977 Nucleation and growth of plagioclase, Makaopuhi and Alae lava lakes, Kilauea Volcano, Hawaii. *Geol. Soc. Am. Bull.* **88**, 78–84.

KRAICHNAN, R. H. 1962 Mixing-length analysis of turbulent thermal convection at arbitrary Prandtl numbers. *Phys. Fluids* **5**, 1374–1389.

MARSH, B. D. 1988 Crystal size distribution (CSD) in rocks and the kinetics and dynamics of crystallization. *Contrib. Min. Petrol.* **99**, 277–291.

MARTIN, D. 1990 Crystal settling and in situ crystallization in aqueous solutions and magma chambers. *Earth Planet. Sci. Lett.* **96**, 336–348.

MARTIN, D. & NOKES, R. 1988 Crystal settling in a vigorously convecting magma chamber. *Nature* **332**, 534–536.

MARTIN, D. & NOKES, R. 1989 A fluid-dynamical study of crystal settling in convecting magmas. *J. Petrol.* **30**, 1471–1500.

RANDOLPH, A. D. & LARSON, M. A. 1971 *Theory of Particulate Processes.* Academic.

RICHTER, F. M. 1978 Experiments on the stability of convection rolls in fluids whose viscosity depends on temperature. *J. Fluid Mech.* **89**, 553–560.

RUDMAN, M. 1992 Two-phase natural convection: implications for crystal settling in magma chambers. *Phys. Earth Planet. Inter.* **72**, 153–172.

SHAW, H. R. 1972 Viscosities of magmatic silicate liquids: an empirical method of prediction. *Am. J. Sci.* **272**, 870–893.

SOLOMATOV, V. S. & STEVENSON, D. J. 1993*a* Suspension in convective layers and style of differentiation of a terrestrial magma ocean. *J. Geophys. Res.* **98**(E3), 5375–5390.

SOLOMATOV, V. S. & STEVENSON, D. J. 1993*b* Kinetics of crystal growth in a terrestrial magma ocean. *J. Geophys. Res.* **98**(E3), 5407–5418.

SPARKS, R. S. J., HUPPERT, H. E., KOYAGUCHI, T. & HALLWORTH, M. 1993 Origin of modal and rhythmic layering by sedimentation in a convecting magma chamber. *Nature* **361**, 246–249.

SPOHN, T., HORT, M. & FISCHER, H. 1988 Numerical simulation of the crystallization of multicomponent melts in thin dikes or sill. 1. The liquidus phase. *J. Geophys. Res.* **93**(B5), 4880–4894.

TAIT, S. R. & JAUPART, C. 1992 Convection and macrosegregation in magma chambers. In *Interactive Dynamics of Convection and Solidification* (ed. S. H. Davis *et al.*), pp. 241–260. Kluwer.

TURNER, J. S. 1979 *Buoyancy Effects in Fluids.* Cambridge University Press.

TURNER, J. S., HUPPERT, H. E. & SPARKS, R. S. J. 1986 Komatiites II. Experimental and theoretical investigations of post-emplacement cooling and crystallization. *J. Petrol.* **27**, 397–437.

WOODS, A. W. & HUPPERT, H. E. 1989 The growth of compositionally stratified solid above a horizontal boundary. *J. Fluid Mech.* **199**, 29–53.